Draft version January 15, 2014
Preprint typeset using LaTeX style emulateapj v. 12/16/11

arXiv:1401.2989v1 [astro-ph.GA] 13 Jan 2014

M31 PIXEL LENSING PLAN CAMPAIGN: MACHO LENSING AND SELF LENSING SIGNALS

S. Calchi Novati[1,2a], V. Bozza[2,3], I. Bruni[4], M. Dall'Ora[5], F. De Paolis[6,7], M. Dominik[8b], R. Gualandi[4], G. Ingrosso[6,7], Ph. Jetzer[9], L. Mancini[10,2], A. Nucita[6,7], M. Safonova[11], G. Scarpetta[1,2,3], M. Sereno[12,13], F. Strafella[6,7], A. Subramaniam[11], A. Gould[14]
(PLAN collaboration)

[1] Istituto Internazionale per gli Alti Studi Scientifici (IIASS), Via Pellegrino 19, 84019 Vietri Sul Mare (SA), Italy
[2] Dipartimento di Fisica "E. R. Caianiello", Università di Salerno, Via Giovanni Paolo II 132, 84084 Fisciano (SA), Italy
[3] INFN, Sezione di Napoli, Via Cinthia 9, 80126 Napoli, Italy
[4] INAF, Osservatorio Astronomico di Bologna, Via Ranzani 1, 40127 Bologna, Italy
[5] INAF, Osservatorio Astronomico di Capodimonte, Salita Moiariello 16, 80131 Napoli, Italy
[6] Dipartimento di Matematica e Fisica "E. De Giorgi", Università del Salento, CP 193, 73100 Lecce, Italy
[7] INFN, Sezione di Lecce, Via Arnesano, 73100 Lecce, Italy
[8] SUPA, University of St Andrews, School of Physics & Astronomy, North Haugh, St Andrews, KY16 9SS, United Kingdom
[9] Institute for Theoretical Physics, University of Zürich, Winterthurerstrasse 190, 8057 Zürich, Switzerland
[10] Max Planck Institute for Astronomy, Königstuhl 17, 69117 Heidelberg, Germany
[11] Indian Institute of Astrophysics, Bangalore 560 034, India
[12] Dipartimento di Scienza Applicata e Tecnologia, Politecnico di Torino, Corso Duca degli Abruzzi 24, 10129 Torino, Italy
[13] INFN, Sezione di Torino, Via Pietro Giuria 1, 10125, Torino, Italy and
[14] Department of Astronomy, Ohio State University, 140 West 18th Avenue, Columbus, OH 43210, US

Draft version January 15, 2014

ABSTRACT

We present the final analysis of the observational campaign carried out by the PLAN (Pixel Lensing Andromeda) collaboration to detect a dark matter signal in form of MACHOs through the microlensing effect. The campaign consists of about 1 month/year observations carried out during 4 years (2007-2010) at the 1.5m Cassini telescope in Loiano ("Astronomical Observatory of BOLOGNA", OAB) plus 10 days of data taken in 2010 at the 2m Himalayan Chandra Telescope (HCT) monitoring the central part of M31 (two fields of about $13' \times 12.6'$). We establish a fully automated pipeline for the search and the characterization of microlensing flux variations: as a result we detect 3 microlensing candidates. We evaluate the expected signal through a full Monte Carlo simulation of the experiment completed by an analysis of the detection efficiency of our pipeline. We consider both "self lensing" and "MACHO lensing" lens populations, given by M31 stars and dark matter halo MACHOs, in the M31 and the Milky Way (MW), respectively. The total number of events is compatible with the expected self-lensing rate. Specifically, we evaluate an expected signal of about 2 self-lensing events. As for MACHO lensing, for full 0.5 (10^{-2}) $M_\odot$ MACHO halos, our prediction is for about 4 (7) events. The comparatively small number of expected MACHO versus self lensing events, together with the small number statistics at disposal, do not enable us to put strong constraints on that population. Rather, the hypothesis, suggested by a previous analysis, on the MACHO nature of OAB-07-N2, one of the microlensing candidates, translates into a sizeable *lower* limit for the halo mass fraction in form of the would be MACHO population, f, of about 15% for 0.5 $M_\odot$ MACHOs.

Subject headings: dark matter — gravitational lensing — galaxies: halos — galaxies: individual (M31, NGC 224) — Galaxy: halo

1. INTRODUCTION

Gravitational microlensing (Roulet & Mollerach 1997) is the tool of choice for the investigation of the dark matter content of galactic halos (Strigari 2013) in form of compact objects (MACHOs). Since the original paper of Paczyński (1986), observational campaigns have been undertaken to this purpose towards the Magellanic Clouds (Moniez 2010), as a probe of the MW halo, and towards the nearby galaxy of Andromeda, M31 (Calchi Novati 2010). Although there is an agreement in excluding that MACHOs can fill up the dark matter halos, some tension remains based on the difficulty to fully disentangle the lensing signal from known (stellar) population ("self lensing") as opposed to the dark matter signal (MACHO lensing).

The EROS (Tisserand et al. 2007) and more recently the OGLE collaboration (Wyrzykowski et al. 2009, 2010, 2011a,b), out of observations towards the Large and Small Magellanic Clouds (LMC and SMC), put rather robust upper limits (at 95% CL) on the halo mass fraction in form of MACHO, f, below 10% up to 1 $M_\odot$ MACHOs (and down to below 5% around 10^{-2} $M_\odot$ objects). On the other hand, the MACHO collaboration had reported a MACHO signal towards the LMC of about $f \sim 20\%$ within the mass range $(0.1 - 1)$ $M_\odot$ (Alcock et al. 2000; Bennett 2005).

To address the reasons of this disagreement the self-lensing scenario, originally discussed in Sahu (1994); Wu (1994); Gould (1995), has been thereafter the object of several analyses (de Rujula et al. 1995; Aubourg et al. 1999; Salati et al. 1999; Alves & Nelson 2000; Gyuk et al. 2000; Jetzer et al. 2002; Mancini et al. 2004; Griest & Thomas

[a] mailto: novati@sa.infn.it
[b] Royal Society University Research Fellow

2005; Calchi Novati et al. 2006, 2009b; Calchi Novati & Mancini 2011; Calchi Novati et al. 2013). Alternative hypotheses have also been discussed, in particular proposing non-standard models of the LMC/SMC which may somehow enhance the expected self-lensing rate (Zaritsky & Lin 1997; Zhao & de Zeeuw 1998; Gould 1998; Evans & Kerins 2000; Zaritsky 2004; Besla et al. 2013).

The main bonus of the line of sight towards M31 (Crotts 1992; Baillon et al. 1993; Jetzer 1994) is that, being an external galaxy, we can fully map its own dark matter halo (roughly, at parity of MACHO mass function and halo fraction, one expects about 2/3 of the MACHO signal, if any, to belong to the M31 halo, with the rest to the MW halo along that line of sight). Because of the large (770 kpc) distance to the sources we enter here the "pixel lensing" regime of microlensing (Gould 1996). In particular, among other specificities, we recall the further degeneracy in the lensing parameter space between the physical event duration, the Einstein time, $t_{\rm E}$ and the impact parameter, u_0, which makes reliable, in most cases, only a determination of the full-width-half-maximum duration, $t_{\rm FWHM}$, (Gould 1996; Wozniak & Paczynski 1997; Gondolo 1999; Alard 2001; Riffeser et al. 2006; Dominik 2009). Additionally, as further addressed below, it results that the ratio of the expected self lensing over MACHO lensing rate is larger with respect to that expected towards the LMC/SMC (quantitatively this depends on the field of view and on the assumed MACHO mass function) and this further complicates the physical interpretation of the data along this line of sight. Indeed, the analysis of the self-lensing signal appears to be at the origin of the disagreement between the POINT-AGAPE collaboration (Calchi Novati et al. 2005), who reported an evidence for a MACHO signal (a different analysis of POINT-AGAPE is discussed in Belokurov et al. 2005), and the MEGA collaboration (de Jong et al. 2006) (but see also de Jong et al. 2004) who concluded that their signal could be fully explained by the expected self-lensing rate (see also the further analyses in Ingrosso et al. 2006, 2007).

Following the difficulty to disentangle the MACHO and the self-lensing signals by considering full sets of events, the detailed analysis of single events turn out to be very important. Interestingly all the analyses of this kind presented up to now, concerning three distinct microlensing candidates towards M31, indicate that the lens should more likely be attributed to the MACHO lensing population (Aurière et al. 2001; Riffeser et al. 2008; Calchi Novati et al. 2010).

The more recently undertaken M31 pixel lensing PAndromeda survey (Lee et al. 2012), which by large overtakes previous ones in term of monitored field of view, baseline extension and cadence (all essential issues to both enhance the expected rate and well characterize the signal) and out of which the detection of 6 new microlensing candidates out of a first analysis of their first year of observation has been reported, promises to mark an important step forward in this framework.

As PLAN collaboration we have undertaken a pixel lensing survey campaign towards M31 based at the Cassini telescope in Loiano (OAB). Following a first pilot season with 11 consecutive nights of observations in 2006 (Calchi Novati et al. 2007), which essentialy probed the feasibility of the project, we have then undertaken a campaign eventually lasted four years, 2007-2010. In 2010 we have extended the monitoring to the 2m Himalayan Chandra Telescope (HCT). The results of the 2007 campaign have been discussed in Calchi Novati et al. (2009a), with the presentation of a fully automated selection pipeline out of which we had selected 2 new microlensing candidates, that we dubbed OAB-N1 and OAB-N2 which we are now going to refer to as OAB-07-N1 and OAB-07-N2, with the additional indication of the year of detection), with OAB-07-N2 being then the object of a further analysis, including that of the lens proper motion (also thanks to additional data kindly provided by the WeCAPP collaboration, Riffeser et al. 2001, 2003), presented in Calchi Novati et al. (2010).

In the present work we intend to present the final analysis of the PLAN survey including all four years of observations, both OAB and HCT data. In particular, we present a third microlensing candidate, already presented in Lee et al. (2012), discuss the expected signal, both self lensing and MACHO lensing, and compare it to the observed rate. In Sect. 2.1 we present the observational data; in Sect. 2.2 we highlight the main steps of data reduction and our photometry procedure; in Sect. 2.3 we outline the method of our automated pipeline and present the results for the search of microlensing candidates; in Sect. 2.4 we discuss our analysis to establish the expected signal: a full Monte Carlo simulation of the experiment completed by an analysis of the detection efficiency of our pipeline; in Sect. 2.5 we present the expected signal and discuss the MACHO lensing versus self-lensing issue as compared to the observed rate; in Sect. 3 we present our conclusions.

2. M31 PLAN PIXEL LENSING SURVEY

2.1. *Observational data*

Most data of our pixel lensing campaign have been collected at the 1.5m Cassini telescope in Loiano, "Osservatorio Astronomico di Bologna" (OAB, http://www.bo.astro.it/loiano/), 785 m above sea level nearby the city of Bologna (Italy). The photometric monitoring was carried out using the "Bologna Faint Object Spectrograph and Camera" (BFOSC) equipped with a CCD EEV LN/1300-EB/1 back illuminated and AR coated, read out noise 3.1 e^-/pixel and gain 2.22 ADU/pixel, pixel scale of 0.58″/pixel and with 1340×1300 pixels for a total field of view of $13' \times 12.6'$. We monitored two fields of view around the inner M31 region, centered at R.A = $0^{\rm h}42^{\rm m}50^{\rm s}$, and decl. = 41°23′57″ (North) and decl. = 41°08′23″ (South), with axes parallel to the south-north and east-west directions, just leaving out the very inner M31 bulge region (Fig. 1). The data have been collected in two broad band filters (similar to Cousin R and I), with exposure times up to 10 minutes per frame depending on the filter and on the moon level. The standard data reduction have been carried out within the IRAF package (http://iraf.noao.edu/).

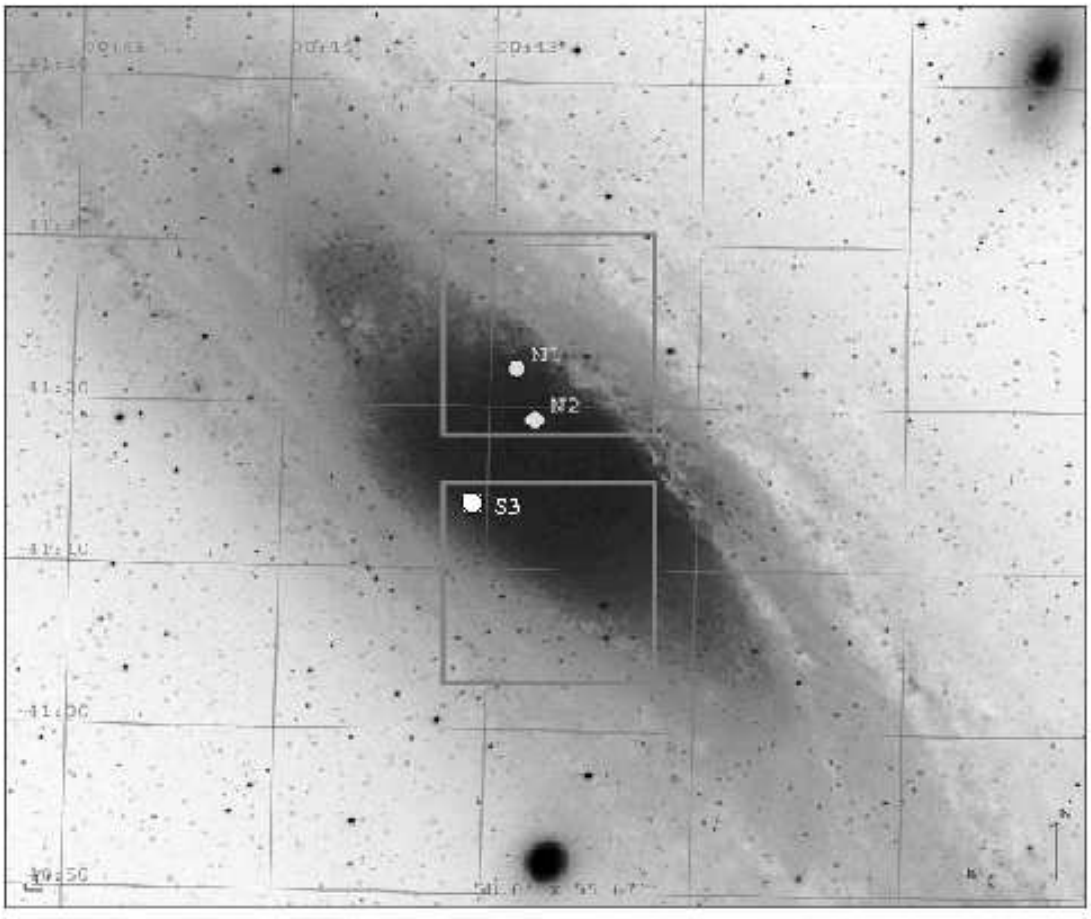

FIG. 1.— Projected on a background archive image of M31 we display the fields of view of the OAB 2007-2010 PLAN pixel lensing campaign and the positions of our 3 microlensing candidates: OAB-07-N1, OAB-07-N2 (Calchi Novati et al. 2009a) and OAB-10-S3, first appeared in Lee et al. (2012) and known as PAnd-4.

The typical microlensing events we expect to detect are relatively faint flux variations (with flux deviation at maximum magnification fainter than about $R \sim 20$) lasting up to a few days. Given the available experimental setup, these features fix our observational requirements. In particular we need a long enough overall baseline with a suitable sampling and high S/N data, namely we ask for full and consecutive nights of observations for an overall period up to about 2 months. The details of the sampling of the first pilot season (2006), whose data are however not further considered in the following, and for the following four years campaign (2007-2010) are reported in Table 1. Overall, the average weather conditions (humidity, cloud coverage) did not turn out to be optimal to our purposes, with our sampling full of unwanted gaps (in particular, the consequence of the non-optimal sampling will be made apparent by the following discussion on the failed microlensing candidate in 2008 and the analysis of the 2010 data below). Indeed, the fraction of at least partially clear nights has remained around 60%, with overall 114 at least partially "good" nights over the 192 allocated ones. Considering however the number of hours we could actually spend observing M31, with an average number of visibility hours given the period of the year and the declination of the site (44°.4 North, almost ideal for observations towards M31) up to almost 10 hours/night, the overall fraction of hours we could monitor M31 with respect to the allocated ones drops to below 40%. Although the quality of the data turned out to be good enough, still we had to reject a sizeable fraction of "bad" images (very poor seeing conditions and/or too high moon level). Specifically, within the selection pipeline we do mask data points with large relative error bars: this further reduced the number of available data points to about 80-90 and 70-80, depending on the light curves, for R and I-band data respectively. This number must be compared to the initial number of awarded nights, 192, for a fraction below 50%. The sky brightness, because of anthropic pollution of the nearby towns, is about 1 mag brighter than in a typical dark site. The typical seeing values were around $2''$ with a strong scatter, though, to further complicate the analysis.

In 2010 we submitted a proposal to carry out parallel observations to those at OAB at the 2m Himalayan Chandra Telescope (HCT) at the Indian Astronomical Observatory (IAO, http://www.iiap.res.in/iao/cycle.html) at 32° North and located at 4500 m above sea level, PI A. Subramaniam, and we were awarded with 10 consecutive nights, October 1-10 (therefore, within the shift allocated at OAB) for 2 hours/night. The photometric monitoring was carried out using the "Himalayan Faint Object Spectrograph and Camera" (HFOSC) equipped with a Thompson CCD with read out noise 4.8 e^-/pixel, gain 1.22 ADU/pixel, pixel scale of $0.296''$/pixel and with 2048×2048 pixels for a total field

TABLE 1
Observational sampling for the 2006-2010 OAB campaign. The first year pilot season is then no longer considered within the analysis.

(1)	(2)	(3)	(4)	(5)
2006	Sep01-Sep11	11	8	4.2
2007	Nov12-Dec31	50[a]	31	3.8
2008	Sep15-Nov23	65[b]	38	4.6
2009	Sep17-Oct22	36	25	5.5
2010	Sep20-Oct31	41[c]	20	4.6
tot		192	114	4.6

Note. — (1): Year; (2): period of the year; (3): number of nights awarded for our project; (4): number of nights with at least some M31 observations; (5): average number of hours/night of M31 observations. In the calculation of the last row the data from the 2006 pilot season are not included. The PI for the 2006 and 2007 proposals was F. Strafella, for the 2008-2010 S. Calchi Novati. In 2010 we have also taken data at the 2m HCT telescope for 10 consecutive days, Oct01-Oct10, PI A. Subramaniam.

[a] 12 consecutive nights have been partly shared with another observer.
[b] 9 not-consecutive nights have been partly shared with other observers and 5 full not-consecutive nights have been allocated to other observers.
[c] 1 full night have been allocated to another observer.

of view of about $10' \times 10'$, slightly smaller than that at OAB. To match with OAB observations we have observed two fields, North and South the M31 center, centered in R.A $= 0^{\rm h}42^{\rm m}50^{\rm s}$ and decl. $= 41°22'57''$ and decl. $= 41°09'23''$, respectively, so to be fully included within the OAB fields of view, with observations evenly distributed in two broad band filters, $R_{\rm C}$ and I. We obtained useful data out of all the 10 scheduled nights, with only some problems of guiding that forced us to reduce the exposure time down to 5 minutes/exposure against the programmed one of 10 minutes/exposure.

2.2. *Data analysis*

The raw data are first reduced with bias and (sky) flat field frames (plus defringing for I band data) using the `ccdred` tasks within IRAF. The photometry is carried out according to the "superpixel" scheme, first introduced within the AGAPE group (Ansari et al. 1997) and further discussed in Calchi Novati et al. (2002, 2009a), which is a fixed-size aperture photometry (we use 5×5 superpixels) with a linear empirical correction to account for the seeing variations. Several images (up to about 20) are taken each night per band and per field. The superpixel light curve is built with a weighted (by the inverse of the square of the flux error) average carried out after the seeing correction so to end up with 1 data point per night per filter. This procedure is suitable to match the expected typical event duration of about a few days.

For the analysis of HCT data, right after the standard CCD reduction, we resample them so to match the OAB pixel scale. To this purpose, first we draw a list of about 300 reference stars per field we use to establish the relative astrometry and then, using the `immatch` tasks within IRAF, we carry out the pixel resampling (moving from the HCT $0.30''$ to the OAB $0.58''$ pixel scale). The rms of the relative astrometry on the resampled HCT images versus the OAB ones is at most of 0.3 pixel. The resampled HCT data are then processed exactly as the OAB data.

2.3. *Pixel lensing pipeline*

The purpose of the pipeline is to establish a list of bona fide microlensing *candidates*. Within this scheme, our specific aim is to build a *fully automated* pipeline. This is crucial to deal with large data set, however the key aspect is that this enables us to reliably estimate the detection efficiency.

The pipeline we use closely follows that described in Calchi Novati et al. (2009a) which we refer to for full details. Hereafter we highlight the relevant steps. We work in the pixel lensing regime so that the search for flux variations is carried out along all the pixels of the image. The analysis is carried out on OAB data working on each year separately. First, we have to establish a list of flux variations. To this purpose we select light curves showing at least 3 consecutive points (one per night) above the baseline level at 3 sigma level, in both R and I band and then ask for the threshold cut, for R band data, $Q > 50$, where Q is the ratio of the χ^2 of a straight line over a Paczyński fit (Calchi Novati et al. 2002, 2003). We recall that each flux variation is spread over a full cluster of nearby pixels whose identification

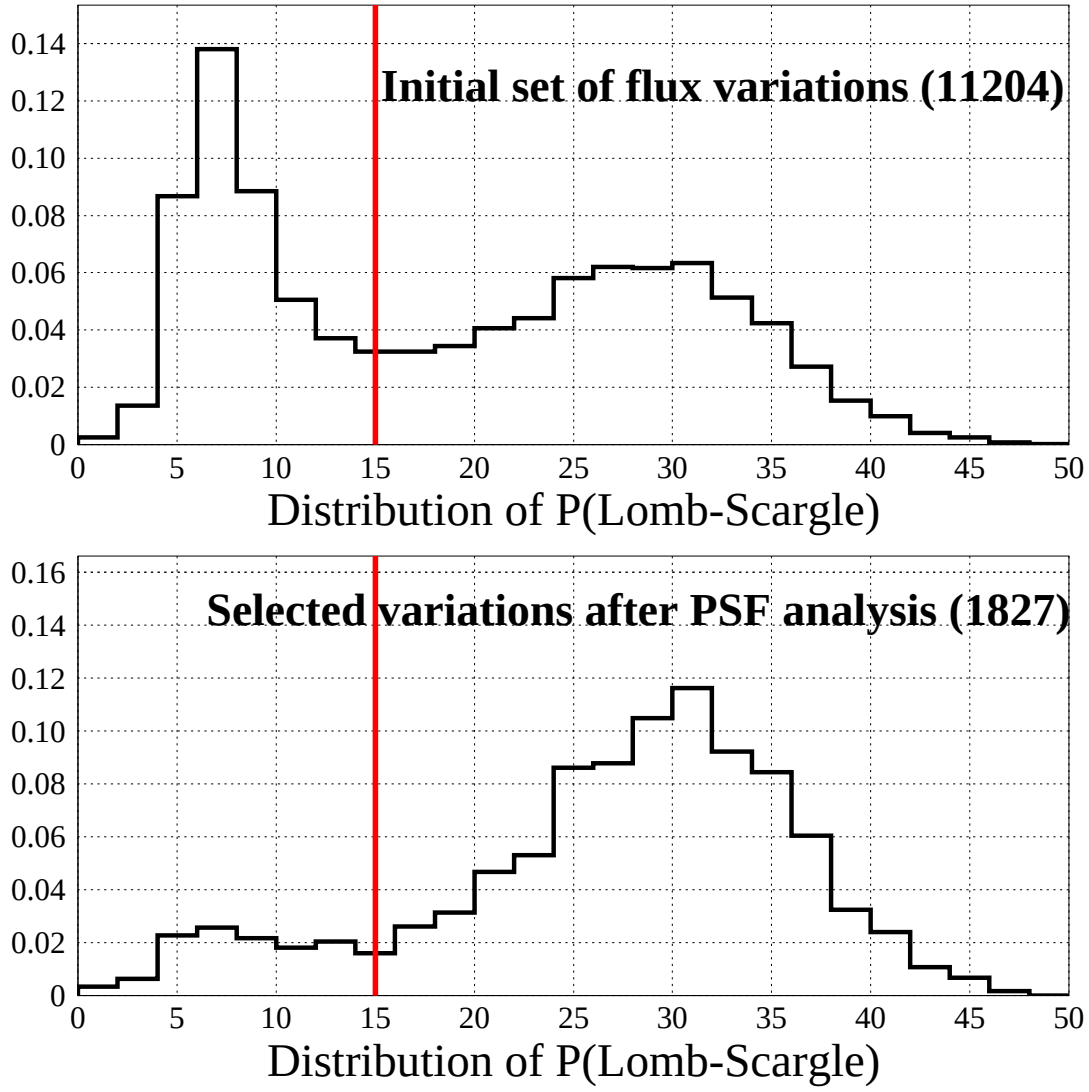
Initial set of flux variations (11204)
Distribution of P(Lomb-Scargle)
Selected variations after PSF analysis (1827)
Distribution of P(Lomb-Scargle)

FIG. 2.— Normalized distribution for the "power", P, of the Lomb-Scargle periodogram analysis on the extension of our selected flux variations on the corresponding INT light curves. Top panel: the full set of initial selected light curves. Bottom panel: the surviving set of selected light curves after the PSF analysis (see text for details). The vertical solid line at $P = 15$ indicates the threshold value used within our selection pipeline.

therefore requires an analysis based on the spatial information of the images (Calchi Novati et al. 2002, 2009a). This way we select a first sample of some 11204 flux variations. As a second step we want to remove all spurious variations (bad pixels, cosmic rays, variations induced by the seeing and so on). To this purpose we study the shape of PSF of the bump on a difference image obtained selecting images at the peak and images along the baseline having similar seeing conditions (Calchi Novati et al. 2009a). This way the number of selected flux variations drops to 1827. Next, we test the stability of the baseline, as indeed we expect most of these variations to be intrinsic variable signals. To this purpose we carry out a Lomb-Scargle periodogram analysis (Lomb 1976; Scargle 1982) that we implement following Press et al. (1992) along three years of INT data (Aurière et al. 2001; Paulin-Henriksson et al. 2003) and consider as a statistics the associated power P. As a threshold value to distinguish between noise and signal we use $P = 15$ (Fig. 2). (As a test that our initial set of 11204 variations is indeed dominated by spurious signals, therefore with most chances to show a stable baseline along the corresponding INT light curve, we find that most of the variations excluded with the PSF analysis have in fact $P < 15$.) Experience (and superpixel photometry) teach us however that this way we may lose bona fide microlensing candidates whose light curve may be superimposed on a (possibly nearby) variable (as the POINT-AGAPE PA-N1 event, Aurière et al. 2001). We therefore allow for flux variations with a variable baseline provided that the flux difference on OAB data be significantly larger than the corresponding one on INT data. The set of flux variations then reduces to 612. Finally we adopt three further selection criteria to constrain the shape of the light curve: the first one for good enough sampling along the flux variations (Calchi Novati et al. 2009a); the second for compatibility with Paczyński, testing the reduced χ^2 and asking $\chi^2 < 10$; the last one for large enough variations,

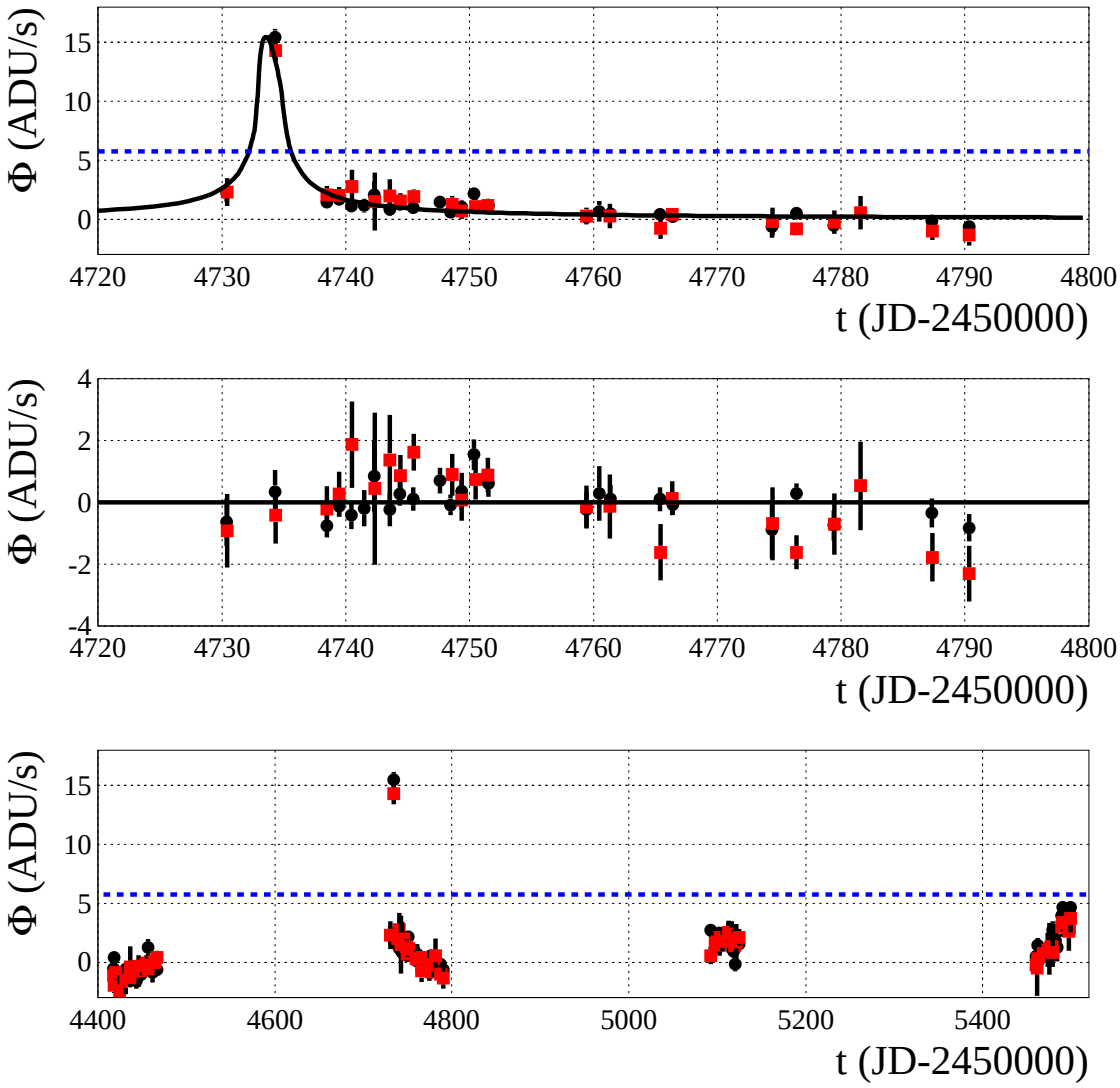

FIG. 3.— The flux variation detected in 2008 on OAB data selected by our automated selection pipeline but finally eliminated from the sample of microlensing candidates (see text for details). Top panel: OAB 2008 light curve with the solid line represents the best Paczyński fit to the data. The dashed horizontal line indicate the flux difference with respect to the baseline corresponding to the flux deviation at maximum of the underlying variable as analysed along the 1999-2001 INT data (see text for details). Middle panel: OAB 2008 light curve of the residuals with respect to the best Paczyński fit. Bottom panel: OAB 2007-2010 light curve and dashed horizontal line as in top panel. All panels: R and I band (rescaled) data are shown with circle and square symbols, respectively. The flux values on the y-axes are rescaled with respect to the R-band values.

with a threshold on the flux difference at maximum magnification expressed in term of magnitude $\Delta R_{\rm max} < 21.5$. This way we are left with 4 microlensing candidate events: OAB-07-N1 and OAB-07-N2 already selected and presented in Calchi Novati et al. (2009a), with the second further discussed in Calchi Novati et al. (2010); a candidate out of 2008 data, further discussed below and finally eliminated from the selection; and, out of the 2010 data, a microlensing candidate already reported by PAndromeda, PAnd-4 (Lee et al. 2012), that we may also dub OAB-10-S3 (N and S stand for North and South, the OAB field where the candidate is located).

The 2008 selected flux variation, in $\alpha, \delta = 0^{\rm h}42^{\rm m}49.22^{\rm s}, 41°22'42.5''$ (J2000.0) at a distance of 6.6′ from the M31 center, with maximum magnification at 4734. (JD-2450000.0), has a very short, half-width-half-maximum duration, $t_{\rm FWHM}$, below 3 days, and a quite bright bump, with flux difference at maximum magnification expressed in term of magnitude $\Delta R_{\rm max} \sim 20.0$ and color $R - I \sim 0.9$ (at the observed peak), Fig. 3. On the other hand, the corresponding extension along the INT light curve show a clear variable signal (with $P = 31$). Indeed, also OAB data (although penalised by a shorter baseline per year of data), in 2008 as well along the full four years of data, show evidence of that variation. A closer astrometry inspection, with rms of the relative OAB-INT astrometry below 0.2 OAB pixel level, reveals that the INT variable sits some 4 INT pixels away from the pixel corresponding to the OAB variations, in a position that coincides with that of the variable identified also on OAB data, 2 OAB pixel away from that of the candidate (OAB and INT pixels cover 0.33″ and 0.58″ respectively, for a distance of the candidate from the underlying

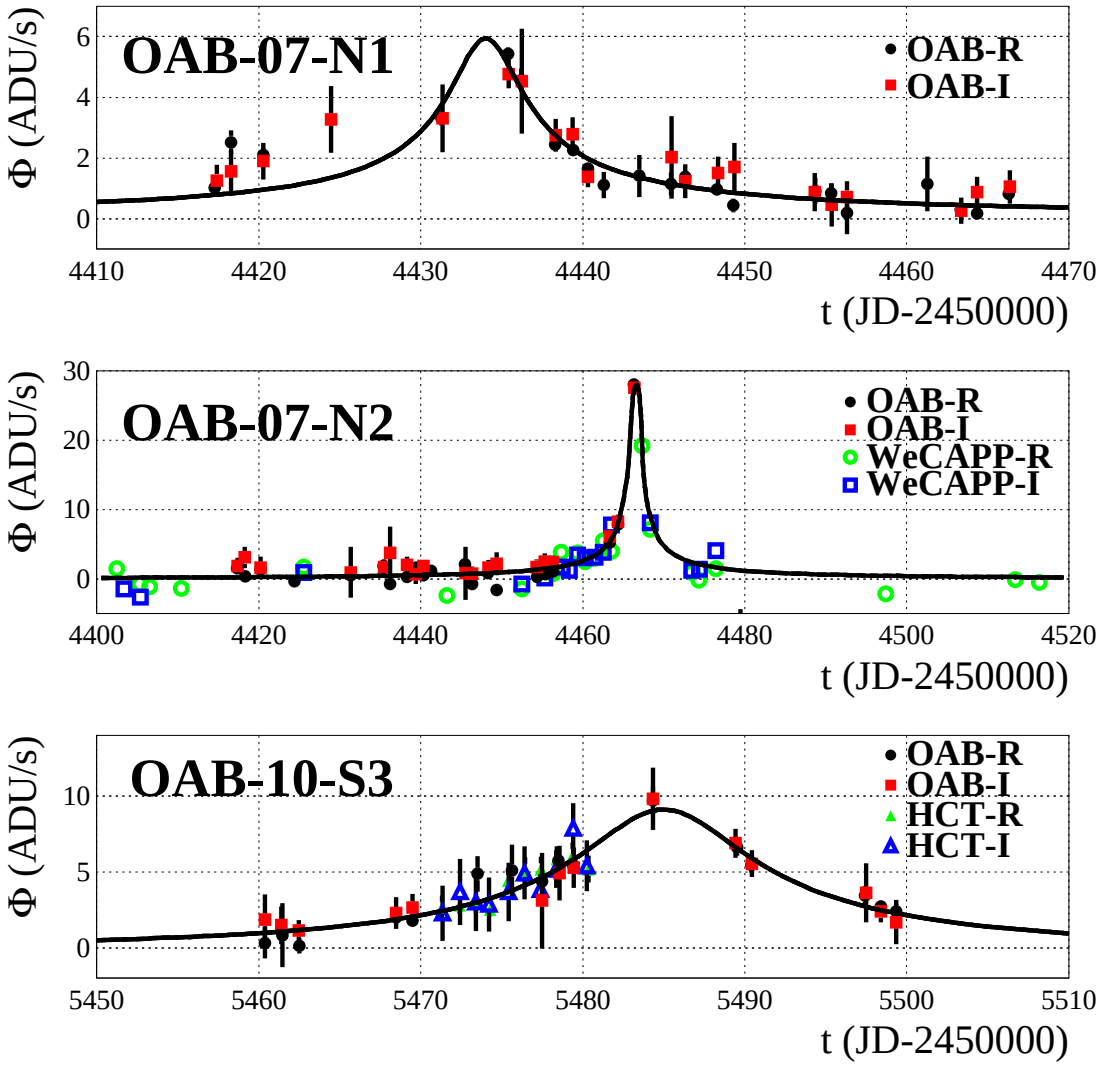

FIG. 4.— Light curves for the three selected microlensing candidate events of our automated selection pipeline. From top to bottom panel: OAB-07-N1 and OAB-07-N2, both first presented in Calchi Novati et al. (2009a), and OAB-10-S3 first published as PAnd-4 in Lee et al. (2012). The solid line represents the best Paczyński fit to the data. Middle and bottom panels: besides the OAB data (filled symbols) we report the additional WeCAPP data also used for the analysis carried out in Calchi Novati et al. (2010); the additional HCT data of our 2010 campaign. The flux values on the y-axes are rescaled with respect to the OAB R-band values expressed in ADU/s.

variable of about 1.2″). The selected flux variation is definitely on a different position with respect to the underlying variable running along the same superpixel light curve of the microlensing candidate. From INT data we infer the color of the variable as $R - I = 1.1$, somewhat redder than the OAB variation, with peak magnitude $R = 21.2$, more than 1 magnitude fainter than the OAB variation. As apparent from inspection of the OAB light curve, the sampling along the bump is poor, with a single data point (in both R and I data, with five images of that night per filter all clearly showing the variation, and with no indications of any trend during the night) well above of the variable baseline and no data, because of bad weather, on the 3 nights immediately before and after the peak. Additionally, a comparison of the two OAB light curves, that centered on the candidate and that centered on the position of the variable, strongly suggest that the flux excess with respect to the baseline for the data points immediately before and after the peak, at the origin of the initial trigger of this flux variation within the selection pipeline, should be attributed to the underlying variable rather than to the candidate which therefore is left with a single significant data point (per band) along the bump. As an initial threshold we ask for three consecutive points, in each band, above the baseline level at 3 sigma level, we are bound to exclude this flux variation, which our available sampling do not enable us to properly characterize, from our selection.

The remaining 3 candidates, on the other hand, all show a stable INT extension light curve (Lomb-Scargle power $P < 7$ for all three of them) as well as a flat baseline on the OAB data on the years off bump. They are further

TABLE 2
Main characteristics of the three candidate microlensing events selected within the fully automated 2007-2010 OAB selection pipeline.

	OAB-07-N1	OAB-07-N2	OAB-10-S3
α (J2000)	$0^{\rm h}42^{\rm m}56.70^{\rm s}$	$0^{\rm h}42^{\rm m}50.36^{\rm s}$	$0^{\rm h}43^{\rm m}11.52^{\rm s}$
δ (J2000)	$41^\circ22'49.8''$	$41^\circ18'40.1''$	$41^\circ13'20.2''$
$\Delta_{\rm M31}$ (arcmin)	7.1	2.8	5.8
t_0 (JD-2450000.0)	4434.0 ± 0.2	4466.1 ± 0.1	5485.1 ± 0.3
$t_{\rm FWHM}$ (days)	7.7 ± 0.7	1.4 ± 0.3	$15. \pm 2.$
$\Delta R_{\rm max}$	21.1 ± 0.1	19.2 ± 0.2	20.6 ± 0.1
$R-I$	1.2 ± 0.1	1.2 ± 0.3	0.8 ± 0.1

Note. — $t_{\rm FWHM}$ and $\Delta R_{\rm max}$ are the duration and the flux difference from the baseline level expressed in term of magnitude according to the fit scheme of Gould (1996). For OAB-07-N1 and OAB-07-N2 the results are slightly different, still compatible within errors, from those reported in Calchi Novati et al. (2009a, 2010) because of the extended baseline. For OAB-07-N2 we report the results of the fit along the joint data sets OAB plus WeCAPP. For OAB-10-S3 we include within the fit the data acquired during our 2010 HCT campaign. OAB-10-S3 has been first published as PAnd-4 in Lee et al. (2012) and we are unable to explain the rather large difference for some of the reported values with respect to those reported in their Tables 3 and 4.

discussed in their respective discovery papers, here we report their main characteristics, Table 2, and show their light curves, Fig. 4.

For the 2010 season we have at our disposal also the additional HCT data set, with a smaller field of view than the OAB one (recovering a fraction of the area of about 60%) and sampled along a 10 consecutive days baseline, about 1/3 of the overall baseline of the OAB 2010 season. PAnd-4/OAB-10-S3 lies within the HCT field of view. However, the last HCT data point falls 4 nights before the peak of the event, still, as the event is rather long the HCT data are still useful as they cover (and nicely overalp with the OAB data, Fig. 4, bottom panel) the rising part and help us to better constrain the event lensing parameters.

As an additional analysis we search for X-ray counterparts of our candidates on archive data. A positive match with a known X-ray source may indeed be an hint of a possible non-microlensing origin of the corresponding optical flux variation. In particular, we cross match our data with both the "M31 Deep *XMM*-Newton Survey X-Ray Source Catalog" (Stiele et al. 2011), an updated version with respect to that we used in our previous analysis (Calchi Novati et al. 2009a), and the Chandra analysis "LMXBs in the bulge of M31" (Voss & Gilfanov 2007). As for the astrometric precision Stiele et al. (2011) report a 3σ positional error for every entry, statistical and systematic, usually around a few arcsec; for the Chandra analysis Voss & Gilfanov (2007) report an indicative range of values, from $0.1''$ to $0.4''$, depending on the brightness of the sources; finally, our astrometric solution is done using about 360 bright stars per field cross-identified with sources in Massey et al. (2006) with (statistical) rms below $0.3''$. The nearest X-ray source to one of our candidates is that lying at $25''$ from OAB-07-N2 (in the Chandra catalog, the nearest in the *XMM*-Newton one is reported at a distance of $27.2''$ with positional error of $1.84''$). For the given errors we can safely rule out an identification. The same conclusion applies, a fortiori, for both OAB-07-N1 and OAB-10-S3. For the first, the nearest source is found at more than $1'$ (both catalogs); for the second at $35.1''$ (Chandra) and $44.4''$ with positional error of $1.83''$ (*XMM*-Newton). The situation is less clear for the 2008 flux variation we have eliminated from our analysis. A positive cross-match of the positions looks plausible if we consider the *XMM*-Newton data, with a source at $5.9''$ with positional error of $4.75''$. This does not hold any more, however, both because of the smaller positional error and the increased distance to our flux variation ($7.5''$), when we look at the Chandra data.

Finally, we may wonder, faced with the large possible variety of microlensing signals (binary lenses and so on), about the impact on our analysis of the requirement of compatibility with a Paczyński shape. If we drop this requirement, we end up with only 2 additional selected flux variations. The first is a clear variable signal, for which we have no available INT data but whose nature is revealed by the analysis of the light curve in the OAB data along the years off bump. The second is a more interesting case: a rather blue, $R-I \sim 0.3$, extremely bright, $\Delta R_{\rm max} \sim 17.6$, variation, located at $\alpha, \delta = 0^{\rm h}43^{\rm m}02.44^{\rm s}, 41^\circ14'10.3''$ (J2000.0), at $3.9'$ from the M31 center, and occurring in 2008 around 4760. (JD-2450000.0) showing several peaks along a time scale of a few days as well as signs of chromaticity. We tried a binary lens fit (Bozza 2010) on this flux variation but we could not find any viable solution. Therefore, we attribute this flux variation to some kind of unidentified cataclysmic variable. As above, we have checked for possible X-ray counterparts. The nearest (bright) source, both the *XMM*-Newton and the Chandra catalogs, lies at about $25''$ and should therefore, for the given errors, be unrelated to this flux variation.

Lee et al. (2012) presented the results of the 2010 season of their PAndromeda (M31) pixel lensing survey. They used a 1.8m telescope with a very wide field of view instrument (7 deg^2) and obtained 91 nights of data along about 5 months in two broad band $r_{\rm P1}$ and $i_{\rm P1}$ filters. In particular they presented results for a search of microlensing events

within the inner $40' \times 40'$ of M31. Overall, they reported six microlensing event candidates. We can use the 2010 PAndromeda results to test our OAB 2010 pipeline. In spite of the very large ratio of ours and the PAndromeda monitored field of view, about 20% considering only the (small) fraction of the overall field of view on which Lee et al. (2012) carried out their microlensing search, as a consequence in fact of the sharp decrease of the expected signal moving outwards from the M31 center, four out of the six PAndromeda candidates falls within the OAB fields of view (PAnd-1,2,3,4). Because of the much longer 2010 PAndromeda baseline, however, only two of these have been detected in October while the OAB campaign was going on (PAnd-1 and 4). As discussed, we find PAnd-4 to coincide with OAB-10-S3 also detected within our pipeline. PAnd-1, which has a very short duration, $t_{\rm FWHM} = 3.1$ d (Lee et al. 2012), unfortunately falls within a gap of the OAB sampling. On the OAB data, along its (short) bump we detect two points, well above 3σ level of the baseline, according to our selection, however, clearly insufficient to characterize, if not even to trigger, a detection. The HCT data span exactly the moment of the PAnd-1 peak, unfortunately, however, PAnd-1 is not included within the HCT field of view. We may therefore conclude that the output of ours and the PAndromeda pipeline are compatible. We consider this conclusion to strengthen the results of the OAB pipeline also for the previous years.

Single bump, achromatic, suitably sampled with large enough S/N, Paczyński-like flux variations can be considered reliable microlensing *candidates*. Excluding binary lenses and/or similar cases where the intrinsic microlensing nature of the event can be accepted beyond any doubt, these flux variations are bound to remain within this limbo. A still possible background is that of cataclysmic variables, which are usually single bump flux variations (at least within the time scale of the usual considered duration for the analysis of the baseline stability). However, these are usually bluer than the typical M31 microlensing candidates, and in particular of those discussed here, and tend to show, as is typical for intrinsic variables, an asymmetry along the flux variation with a sharper rising part. For the case under examination, the intrinsic microlensing nature of two of the reported flux variations is further supported by additional data by WeCAPP, for OAB-07-N2, and HCT (presented here) and PAndromeda for OAB-10-S3. Indeed, the simultaneous detection on multiple pipelines and/or multiple data sets of the same flux variation, even if by itself can not be taken as a proof of the genuine microlensing nature of the flux variation, may make us more confident on its interpretation. This is for two main reasons. First, the joint analysis with additional data may further constrain the microlensing parameter space. Second, each pipeline (a fortiori with a different data set), in its broadest sense (data reduction, photometric analysis, flux variation search and characterization), comes with its own systematics which tend to be ruled out by multiple detections. More specifically, in Calchi Novati et al. (2009a) with OAB data alone OAB-07-N2 was not fully sampled and we could only put forward a guess on its microlensing nature. The joint analysis with the additional WeCAPP data then enabled us (Calchi Novati et al. 2010) to probe the symmetric and achromatic shape of the full flux variation then confirming the microlensing interpretation. Furthermore, the dense sampling made possible a much more refined analysis of the microlensing parameter space. Indeed, together with an additional analysis on the underlying source flux on archival data, the joint OAB plus WeCAPP light curve enabled us to conclude, even if only marginally, through a study of the lens proper motion (Gould 1994; Han & Gould 1996), in favor of the MACHO nature of the lens. As for OAB-10-S3, the HCT data presented here, even if not necessary to enhance its detection, enabled us a better characterization of the microlensing parameters. This flux variation enjoys then of being selected as a microlensing candidate by two completely independent pipelines (on different data sets), specifically, besides the present one, also by PAndromeda as PAnd-4 (Lee et al. 2012). For purposes of the following analysis we therefore will consider the three flux variations selected within our pipeline as *bona fide* microlensing variations.

2.4. *Monte Carlo and efficiency analyses*

For the analysis of the expected signal we closely follow the scheme outlined in Calchi Novati et al. (2009a) and references therein which we refer to for full details. First, we build a Monte Carlo simulation (based on the original work in Baillon et al. (1993); Ansari et al. (1997)) where, on top of the astrophysical model of all the quantities of interest we simulate the microlensing flux variations. The evaluation of the expected signal for a microlensing experiment is based of the microlensing *rate* (Griest 1991; Calchi Novati et al. 2008), with the specific case of M31 pixel lensing also discussed in Han (1996); Baltz & Silk (2000); Gyuk & Crotts (2000); Kerins et al. (2001); Riffeser et al. (2006). Our model of M31 is based on the Kent (1989) data. For both M31 bulge and disk stars, we make use of a synthetic luminosity function extracted from IAC-star (Aparicio & Gallart 2004) with sources expected up to a magnitude of roughly $M_I \sim 2$. Finally, the flux variations are simulated as single-lens microlensing events accounting for finite source size (Witt & Mao 1994) and we reproduce the observational conditions, in particular the sampling, of our OAB campaign. Within the Monte Carlo we carry out a first (knowingly over-optimistic) selection pipeline asking for the flux variations to have at least 3 consecutive points 3 sigma above the baseline level. Monte Carlo selected light curves may however not be selected within our data set. Within the Monte Carlo we can not in particular reproduce those steps of our pipeline where the spatial information across the images comes into play: the cluster analysis we carry out to identify the initial set of flux variations and the PSF analysis we use to exclude spurious signals; additionally, within the Monte Carlo we do not reproduce all the problems intrinsic to the images such as crowding, background flux variations due to underlying variables and so on: all these aspects must however be taken into account. To get to a reliable estimate of the expected signal we therefore inject, making use of the `daophot` tasks within IRAF, (part) of these Monte Carlo selected light curves on the real data (R band only), just after the basic CCD reduction, and then run our selection pipeline from scratch. Finally, as a result, we end up with the distributions of the parameters and the number of events for the expected signal. As lens populations we consider M31 bulge and lens stars ("self-lensing") and

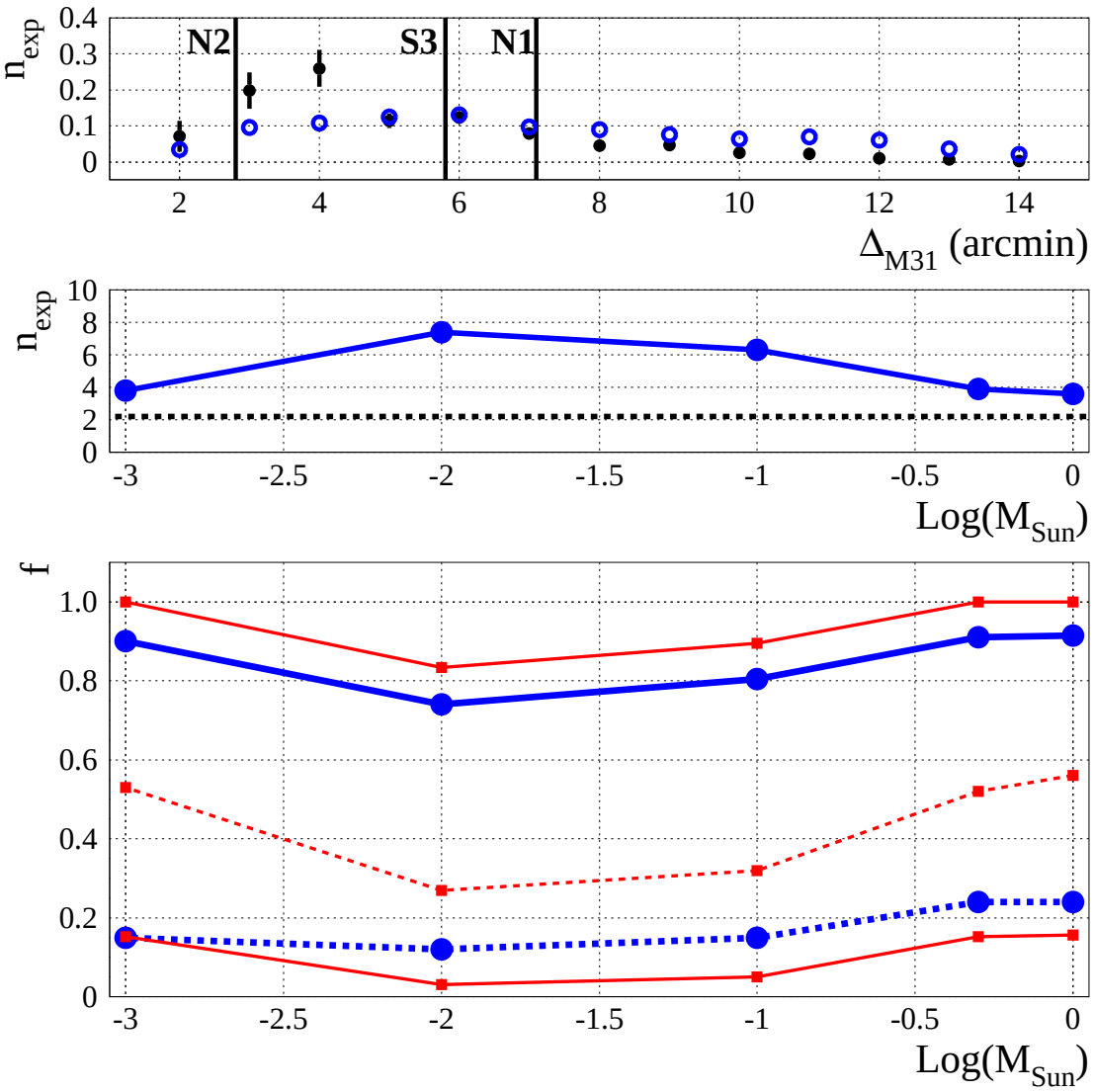

FIG. 5.— Top panel: the (normalized) expected number of events for self lensing (filled symbols) and MACHO lensing as a function of the distance to the M31 center (arcmin). The (statistical) error bars appear only when they exceed the size of the symbols. The solid vertical lines indicates the position within this parameter space of the selected candidates. Middle panel: the number of expected MACHO lensing events, for full (M31 and MW) halos ($f = 1$) as a function of the (logarithm of the) MACHO mass; the horizontal dashed line indicates the expected number of self-lensing events. Bottom panel: limits on the halo mass fraction in form of MACHOs, f, as a function of the (logarithm of the) MACHO mass obtained from a Bayesian analysis based on the evaluation of the likelihood comparing the expected, MACHO and self lensing, signal to the 3 observed events (see text for details). Circle symbols: modal values (dashed lines) and upper 95% CL limit in the case where no a priori hypotheses are made on the nature of the observed events. Square symbols (and thin lines): modal values (dashed lines) and upper and lower 95% CL limits obtained under the additional hypothesis that, following the analysis in Calchi Novati et al. (2010), OAB-07-N2 *is* a MACHO lensing event.

MACHO lensing as MACHOs belonging to the M31 and MW halos, for which we study a set of delta mass functions within the range $10^{-3} - 1$ $M_\odot$. Specifically, to minimize the statistical noise on the number of expected events, within the Monte Carlo we simulate 10^9 events for self lensing and as much for each mass of MACHO lensing, per year. Out of the selected events within the Monte Carlo we then inject 12000 events for self lensing and for each MACHO mass value per year (to avoid overlaps among the injected events on the images we split the analysis so to have 500 events per field for each run).

2.5. *The statistics on MACHOs*

The driving astrophysical question of the present analysis is the content in MACHOs of galactic halos. It is therefore of primarily interest to address the issue of the *nature* of the observed events, whether self lensing or MACHO. Besides the already discussed and peculiar case of OAB-07-N2, the main statistics at our disposal, also considering the power of investigation within the detection efficiency analysis, are the magnitude at maximum and the color, which at most can be used to assess the coherence of the analysis with the expected signal with no reference however to the specific lens population, the duration and the position. As for the duration, $t_{\rm FWHM}$, we recall from previous analyses

(Kerins et al. 2001; Calchi Novati et al. 2005; Riffeser et al. 2006), and specifically for the OAB data our analysis in Calchi Novati et al. (2009a), that most events are expected, as indeed we find, to last less than about 10-20 days, but this parameter is unfit to distinguish among the lens populations, at least for those of roughly equal lens mass (thus, specifically, for stellar lenses and MACHOs around 0.5 $M_\odot$) for which one would rather need a reliable estimate of the Einstein time. On the other hand, the small number of events at our disposal makes the position of the events of limited use to this purpose, moreover it should be recalled that the analysis of the originally proposed signature of M31 MACHO lensing versus self lensing due to the M31 disk inclination may in fact be complicated by effects of differential extinction (An et al. 2004; Montalto et al. 2009). Still, self-lensing events tend to be more clustered than MACHOs around the M31 center, and specifically this holds for our experimental configuration (Calchi Novati et al. 2009a). In fact, this is the underlying motivation, in the following likelihood analysis, for binning the space in unit of distance from the M31 center (Fig. 5, top panel). The main statistics to disentangle MACHO and self lensing signals which is left is therefore the expected *number* of events. The results of our analysis, Monte Carlo simulation followed by the efficiency analysis, are as follows. For self lensing we expect 2.2 ± 0.2 events. For MACHO lensing, for full (f=1) M31 and MW halos, from about 4 up to above 7 events, according to the mass value (Fig. 5, middle panel) and with statistical relative error around 10%, with a maximum for the expected signal at 10^{-2} $M_\odot$ before a decrease, for 10^{-3} $M_\odot$, due to the drop of sensitivity for very short duration events related to our (insufficient) sampling. The reported *statistical* error is that associated to the Monte Carlo simulation, for which the (Poisson) error scales as the square root of the simulated events (Section 5.1 of Calchi Novati et al. 2005) with the final budget dominated by large by the error on the efficiency. Next, we may compare this result for the expected signal with $n_{\rm obs} = 3$ observed events with the additional information, as already recalled, that OAB-07-N2 may indeed be rather a MACHO than self lensing. Leaving aside this information for the moment, the conclusion of the analysis, based on the bare numbers, is that self lensing is fully able to explain the observed rate. Specifically, according to the Poisson statistics followed by the number of events, for the given expected mean signal (and excluding for a moment the MACHO signal), the 95% CL upper limit is for 6.3 events, well above the observed rate. We have then to consider the expected MACHO lensing. Here a fundamental remark is that the expected signal, for *full* halos, is not much larger than the self lensing one. Together, these results suggest that the current experiment is unable to set lower limits to MACHOs and to establish, if any, only rather weak upper limits. On the other hand, that same smallness of the expected MACHO lensing signal renders, as soon as we acknowledge the MACHO nature of even only one event, as we may do for OAB-07-N2 according to the analysis in Calchi Novati et al. (2010), the situation altogether different as we may expect at once to find a sizeable *lower* limit for the halo mass fraction in form of MACHOs.

We can quantify the above statements by inferring from the data a probability distribution for f through a Bayesian analysis based first on the evaluation of the likelihood function. To this purpose we closely follow the approach outlined in Calchi Novati et al. (2005) (for a specific discussion on the use of the likelihood within a microlensing analysis we also refer to Calchi Novati et al. 2013). We bin the entire field of view into $N_{\rm bin}$ bins, for each we have the model prediction x_i ($i = 1, \ldots, N_{\rm bin}$) and the observed number of events n_i. For fixed model, the different x_i are not independent as they all depend on the halo fraction, f,

$$x_i\,(f, m) = b_i + f s_i\,(f = 1, m)\ , \tag{1}$$

with m being the MACHO mass and where the *signal* we look for, s, is the number of MACHO events, the *background*, b, being the self lensing signal (as our purpose is to constrain f we may rather refer to the signal as the product $f \cdot s$). The likelihood is the product of the individual probabilities of the n_i in each bin

$$L\,(n_i|x_i) = \prod_{i=1}^{N_{\rm bin}} \frac{1}{n_i!} \mathrm{e}^{-x_i} x_i^{n_i} = \mathrm{e}^{-N_{\rm exp}} \prod_{i=1}^{N_{\rm obs}} x_i\,, \tag{2}$$

where in the second step we have specialised the bins to contain either 0 or 1 observed event (Gould 2003). As previously addressed, for binning, we choose the distance from the M31 center, and we use $1'$ bins. Keeping the MACHO mass fixed as a parameter, for a flat prior for f different from zero in the interval $(0, 1)$, given the likelihood we can then evaluate the probability distribution $P(f)$. We evaluate the modal value for f and, around it, the 95% CL region which then defines the lower and the upper limits. The results of this analysis are shown in Fig. 5, bottom panel. If we do not introduce any prior within the analysis, as anticipated, the observed signal turn out to be compatible with the expected self lensing rate, with no lower limits for f and upper limits above 70% (90% in the range 0.5-1 $M_\odot$). If instead we impose that OAB-07-N2 *is* a MACHO, namely within Eq. 1 we set the self-lensing background to zero, $b = 0$, we find a, sizeable, 15% *lower* limit for f in the mass range 0.5-1 $M_\odot$, with no upper limit and somewhat smaller limits moving down to $10^{-2} M_\odot$. Finally, the observed rate (3 events) is in fact also compatible with no self lensing (for an expected signal of 2.2 events). If we assume this extreme case as a working hypothesis the lower limit for f in the mass range 0.5-1 $M_\odot$ would rise to about 30%.

3. CONCLUSION

We have presented the final analysis of the 4-years, 2007-2010, pixel lensing campaign of the PLAN collaboration towards M31 aimed at the search and the characterization of microlensing events. The driving scientific motivation is the search for a dark matter signal in galactic halos in form of compact objects, MACHOs. The specific aim of the campaign is to better understand the signal coming from the putative MACHO population as compared to the

background signal of self-lensing events, defined as opposed to MACHO lensing with the lens belonging to known stellar (M31) populations. To this purpose we monitored the central region of M31, where the expected rate is larger for both signals, still with self lensing expected to be more clustered around the M31 center, looking for new microlensing events. A key aspect of our analysis is the use of a full automated pipeline for the search of microlensing-like flux variations which, besides leading us to the determination of a set of microlensing candidates, enables us to reliably estimate the detection efficiency. For a given astrophysical model this eventually enables us to reliably estimate the expected signal through a Monte Carlo simulation of the experiment.

The analysis is based on data collected at the 1.5m telescope of the Astronomical Observatory of Bologna (OAB) in two broad R and I-bands in two fields $13' \times 12.7'$ around the M31 center. After a first year pilot season (2006) (Calchi Novati et al. 2007) the observational campaign eventually lasted four years (2007-2010) with an awarded baseline to our survey, on average, of some 48 night/year plus, in 2010, 10 consecutive nights of complementary data from the 2m Himalayan Chandra Telescope (HCT). Altogether, however, bad weather and/or generally unsuitable observational conditions introduced several gaps within our sampling with the final analysis based on the data collected, overall, during about 90 nights (excluding the contribution of HCT data). The expected short duration of the microlensing flux variations together with the small rate of events magnify the impact of this problem. Indeed, this is made explicit also from the analysis presented in this paper. We have discussed the case of a flux variation preliminarly selected, in the 2008 season, but finally rejected because of incomplete sampling along the bump. For the same reason we did not select the microlensing candidate PAnd-1 (Lee et al. 2012) even if included within our field of view and baseline.

The results of the pipeline are as follows. Overall, we select three microlensing candidate events: OAB-07-N1 and OAB-07-N2, both first presented in Calchi Novati et al. (2009a), and a third candidate occurred during the 2010 season and already published by PAndromeda in Lee et al. (2012) as PAnd-4, which we also dub OAB-10-S3, and for which we also have data from HCT. The results of our pipeline for the 2010 season turns out to be compatible with those of PAndromeda (Lee et al. 2012) (thus strengthening its conclusions also for the previous seasons). As discussed within the text, the detection of the same flux variation on multiple pipelines and/or data sets is useful for the purpose of its interpretation as a microlensing candidate. First, additional data may help to better constrain the candidate microlensing parameter space. Second, any independent detection comes with the bonus of removing, if any, the systematics of each pipeline. Besides the case of OAB-10-S3 (PAnd-4) we recall OAB-07-N2, first presented in Calchi Novati et al. (2009a), of which we could then perform a new analysis thanks to additional WeCAPP data (Calchi Novati et al. 2010). In particular, these made possible a refined analysis of the lensing parameter space, specifically of the lens proper motion, which enabled us to conclude in favor of the MACHO nature of the lens. For purposes of the analysis we consider all three candidates as *bona fide* microlensing variations.

The observed rate, based on the *number* of events, is compatible with the expected self-lensing signal. A major outcome of our analysis, though, is that the expected MACHO lensing, for full M31 and MW halos, is only marginally larger than self lensing, which is a different situation from analyses towards the Magellanic Clouds where the expected self-lensing signal is evaluated to be much smaller than that of MACHO lensing. This result, together with our small statistics of events at disposal, prevents us from drawing strong constraints on the putative MACHO population. This situation makes extremely important, whenever possible, the detailed analysis of single events addressing the issue of their nature, as was the case for the event POINT-AGAPE-S3/WeCAPP-GL1 (Riffeser et al. 2008), and as we could do for OAB-07-N2 (Calchi Novati et al. 2010). Indeed, the hypothesis on the MACHO nature of OAB-07-N2, as suggested by that last analysis, drives a sizeable lower limit for the halo mass fraction in form of MACHOs, f. Quantitatively, we evaluate an expected self lensing signal of 2.2 events, fully compatible therefore with our 3 observed events, and a MACHO lensing, for full halos, of 4-7 events moving through our chosen range of masses ($10^{-3} - 1$ M$_\odot$). In particular we evaluate an expected signal of 3.9 events for 0.5 M$_\odot$ which, under the hypothesis that OAB-07-N2 is a MACHO, translates into a lower limit for f of about 15%. This outcome makes apparent the need of carrying out similar analyses using larger sets of events, possibly across larger fields of view, for which, besides their number, also additional statistics may be used to disentangle the MACHO from the self lensing signal. In this perspective, the observational campaign PAndromeda (Lee et al. 2012) promises to mark an important further step into the understanding of this issue.

We thank M. Fitzpatrick for his support with IRAF. AG was supported by NSF grant AST-1103471. MD is thankful to Qatar National Research Fund (QNRF), member of Qatar Foundation, for support by grant NPRP 09-476-1-078. PJ acknowledges support by the Swiss National Science Foundation.

REFERENCES

Alard, C. 2001, MNRAS, 320, 341
Alcock, C., et al. 2000, ApJ, 542, 281
Alves, D. R., & Nelson, C. A. 2000, ApJ, 542, 789
An, J. H., et al. 2004, MNRAS, 351, 1071
Ansari, R., et al. 1997, A&A, 324, 843
Aparicio, A., & Gallart, C. 2004, AJ, 128, 1465
Aubourg, É., Palanque-Delabrouille, N., Salati, P., Spiro, M., & Taillet, R. 1999, A&A, 347, 850
Aurière, M., et al. 2001, ApJ, 553, L137
Baillon, P., Bouquet, A., Giraud-Heraud, Y., & Kaplan, J. 1993, A&A, 277, 1
Baltz, E. A., & Silk, J. 2000, ApJ, 530, 578
Belokurov, V., et al. 2005, MNRAS, 357, 17
Bennett, D. P. 2005, ApJ, 633, 906
Besla, G., Hernquist, L., & Loeb, A. 2013, MNRAS, 428, 2342
Bozza, V. 2010, MNRAS, 408, 2188
Calchi Novati, S. 2010, General Relativity and Gravitation, 42, 2101, Invited Review
Calchi Novati, S., et al. 2009a, ApJ, 695, 442

Calchi Novati, S., et al. 2007, A&A, 469, 115
Calchi Novati, S., et al. 2010, ApJ, 717, 987
Calchi Novati, S., de Luca, F., Jetzer, P., Mancini, L., & Scarpetta, G. 2008, A&A, 480, 723
Calchi Novati, S., De Luca, F., Jetzer, P., & Scarpetta, G. 2006, A&A, 459, 407
Calchi Novati, S., et al. 2002, A&A, 381, 848
Calchi Novati, S., Jetzer, P., Scarpetta, G., Giraud-Héraud, Y., Kaplan, J., Paulin-Henriksson, S., & Gould, A. 2003, A&A, 405, 851
Calchi Novati, S., & Mancini, L. 2011, MNRAS, 416, 1292
Calchi Novati, S., Mancini, L., Scarpetta, G., & Wyrzykowski, Ł. 2009b, MNRAS, 400, 1625
Calchi Novati, S., Mirzoyan, S., Jetzer, P., & Scarpetta, G. 2013, MNRAS, 435, 1582
Calchi Novati, S., et al. 2005, A&A, 443, 911
Crotts, A. P. S. 1992, ApJ, 399, L43
de Jong, J. T. A., et al. 2004, A&A, 417, 461
de Jong, J. T. A., et al. 2006, A&A, 446, 855
de Rujula, A., Giudice, G. F., Mollerach, S., & Roulet, E. 1995, MNRAS, 275, 545
Dominik, M. 2009, MNRAS, 393, 816
Evans, N. W., & Kerins, E. 2000, ApJ, 529, 917
Gondolo, P. 1999, ApJ, 510, L29
Gould, A. 1994, ApJ, 421, L71
Gould, A. 1995, ApJ, 441, 77
Gould, A. 1996, ApJ, 470, 201
Gould, A. 1998, ApJ, 499, 728
Gould, A. 2003, ApJ, 583, 765
Griest, K. 1991, ApJ, 366, 412
Griest, K., & Thomas, C. L. 2005, MNRAS, 359, 464
Gyuk, G., & Crotts, A. 2000, ApJ, 535, 621
Gyuk, G., Dalal, N., & Griest, K. 2000, ApJ, 535, 90
Han, C. 1996, ApJ, 472, 108
Han, C., & Gould, A. 1996, ApJ, 467, 540
Ingrosso, G., Calchi Novati, S., de Paolis, F., Jetzer, P., Nucita, A. A., Scarpetta, G., & Strafella, F. 2007, A&A, 462, 895
Ingrosso, G., Calchi Novati, S., de Paolis, F., Jetzer, P., Nucita, A. A., & Strafella, F. 2006, A&A, 445, 375
Jetzer, P. 1994, A&A, 286, 426
Jetzer, P., Mancini, L., & Scarpetta, G. 2002, A&A, 393, 129
Kent, S. M. 1989, AJ, 97, 1614
Kerins, E., et al. 2001, MNRAS, 323, 13
Lee, C.-H., et al. 2012, AJ, 143, 89
Lomb, N. R. 1976, Ap&SS, 39, 447
Mancini, L., Calchi Novati, S., Jetzer, P., & Scarpetta, G. 2004, A&A, 427, 61
Massey, P., Olsen, K. A. G., Hodge, P. W., Strong, S. B., Jacoby, G. H., Schlingman, W., & Smith, R. C. 2006, AJ, 131, 2478
Moniez, M. 2010, General Relativity and Gravitation, 42, 2047, Invited Review
Montalto, M., Seitz, S., Riffeser, A., Hopp, U., Lee, C.-H., & Schönrich, R. 2009, A&A, 507, 283
Paczyński, B. 1986, ApJ, 304, 1
Paulin-Henriksson, S., et al. 2003, A&A, 405, 15
Press, W. H., Teukolsky, S. A., Vetterling, W. T., & Flannery, B. P. 1992, Numerical recipes in FORTRAN. The art of scientific computing (Cambridge: University Press, —c1992, 2nd ed.)
Riffeser, A., Fliri, J., Bender, R., Seitz, S., & Gössl, C. A. 2003, ApJ, 599, L17
Riffeser, A., et al. 2001, A&A, 379, 362
Riffeser, A., Fliri, J., Seitz, S., & Bender, R. 2006, ApJS, 163, 225
Riffeser, A., Seitz, S., & Bender, R. 2008, ApJ, 684, 1093
Roulet, E., & Mollerach, S. 1997, Phys. Rep., 279, 67
Sahu, K. C. 1994, Nature, 370, 275
Salati, P., Taillet, R., Aubourg, É., Palanque-Delabrouille, N., & Spiro, M. 1999, A&A, 350, L57
Scargle, J. D. 1982, ApJ, 263, 835
Stiele, H., Pietsch, W., Haberl, F., Hatzidimitriou, D., Barnard, R., Williams, B. F., Kong, A. K. H., & Kolb, U. 2011, A&A, 534, A55
Strigari, L. E. 2013, Phys. Rep., 531, 1
Tisserand, P., et al. 2007, A&A, 469, 387
Voss, R., & Gilfanov, M. 2007, A&A, 468, 49
Witt, H. J., & Mao, S. 1994, ApJ, 430, 505
Wozniak, P., & Paczynski, B. 1997, ApJ, 487, 55
Wu, X.-P. 1994, ApJ, 435, 66
Wyrzykowski, Ł., et al. 2010, MNRAS, 407, 189
Wyrzykowski, Ł., et al. 2009, MNRAS, 397, 1228
Wyrzykowski, Ł., et al. 2011a, MNRAS, 413, 493
Wyrzykowski, L., et al. 2011b, MNRAS, 416, 2949
Zaritsky, D. 2004, ApJ, 614, L37
Zaritsky, D., & Lin, D. N. C. 1997, AJ, 114, 2545
Zhao, H., & de Zeeuw, P. T. 1998, MNRAS, 297, 449